BL4A2

Fabrication of Electrode Holes on the Supported Membrane Biosensor Substrates by Femto-Second Laser Patterning Followed by SR Etching

M.M. Rahman[1], R. Sasaki[2], H. Nagai[2], M. Yoshida[2], M. Aoyama[3], T. Yano[3], H. Uno[3], R. Tero[3], Y. Nonogaki[1,3] , T. Urisu [1,3]

[1] *Graduate University for Advanced Studies, Myodaiji, Okazaki 444-8585, Japan*
[2] *AISHIN SEIKI Co., Ltd. 17-1 Kojiritsuki, Hitotsugi-cho, Kariya 448-0003, Japan*
[3] *Institute for Molecular Science , NINS, Myodaiji, Okazaki 444-8585, Japan*

Introduction

The supported membrane is a single lipid bilayer supported on a solid surface, and is useful as artificial cell membranes for the study of biological reactions of membrane proteins. We are developing supported membrane biosensors from the interest in developing the new research tool of the cell membrane surface reactions, and these devices are interesting also from the view point of application to the large scale screening method for the new medicine development.

In the present work, we have fabricated very flat Si substrates with buried-electrodes having the structure of SiO_2/$CoSi_2$/Si(100)/$CoSi_2$/Au by the thin film deposition using of sputtering and the electrode hole fabrication using the femto-second laser patterning followed by synchrotron radiation (SR) etching.

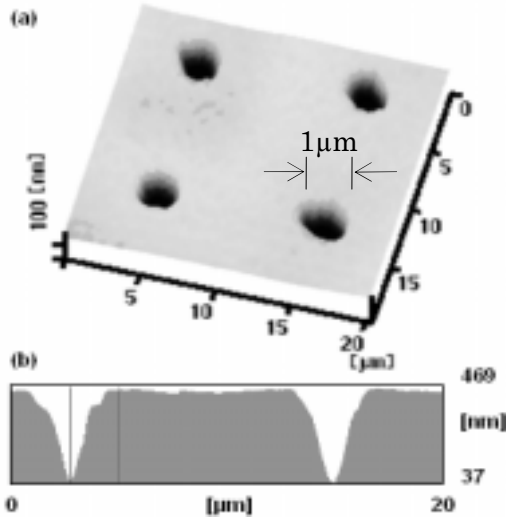

Fig. 1 AFM image (20x20 μm^2) and the cross section of the SiO_2 surface electrode hole fabricated by femto-second laser and SR etching.

Results and Discussion

Co thin film (200nm) was deposited on the SiO_2/$CoSi_2$/Si(100)/$CoSi_2$/Au substrates and small hole patterns were fabricated by the femto second laser pulses. These hole patterns were used as the contact mask of the SR-stimulated etching. SR was used because of its unique features of high spatial resolution, extremely high material selectivity between $CoSi_2$ and SiO_2, low damage, and clean etching atmosphere. There are lot of advantages such as process simplicity compared with the electron beam (EB) lithography and no contamination by beam elements compared with focused ion beam patterning. Then SR etching using SF_6 (0.05 torr) + O_2 (0.002 torr) reaction was used for the etching of SiO_2 using the Co contact mask. Etching stopped at the thin electrode ($CoSi_2$) surface. After the removal of Co mask with 0.1 M HNO_3 aq, AFM images showed that the surface was very flat (Rz=1.5 nm) as shown in Fig. 1.

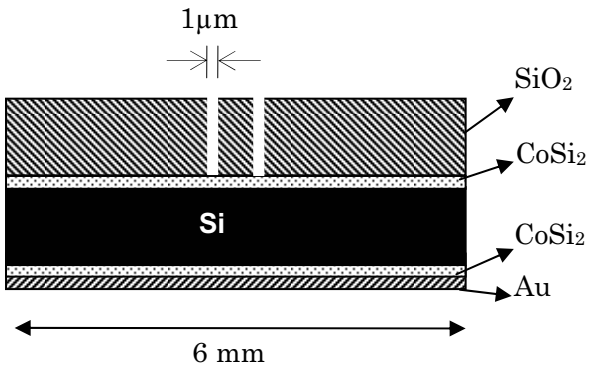

Fig. 2 A schematic illustration for the biosensor substrate.

BL4B

X-Ray Magnetic Circular Dichroism Study on Cu Capping on Ultrathin Ni Films Grown on Clean and O-Adsorbed Cu(001) Surfaces

T. Nakagawa, H. Watanabe, T. Yokoyama

Department of Molecular Structure, Institute for Molecular Science, Okazaki 444-8585 Japan

Ultrathin Ni/Cu(001) films are well known to show unique magnetic properties. The spin reorientation transition (SRT) occurs twice by varying the Ni thickness; at <9 ML (monolayer) the easy axis is in plane, at 9-40 ML it is perpendicular, and at >40 ML it is again in plane. In this work, we have studied the Cu capping effect on the Ni films grown on clean and O-preadsorbed Cu(001) by means of in-laboratory magneto-optical Kerr effect (MOKE) and UVSOR x-ray magnetic circular dichroism (XMCD) methods.

Experiments

Ni was deposited on clean (1×1) and O-pre-adsorbed (2√2×√2)R45° Cu(001) at room temperature in ultrahigh vacuum chambers. The thickness was monitored with the RHEED oscillations. Cu was subsequently deposited on Ni/Cu(001). Ni *L*-edge XMCD was taken at BL4B [1] at ~100 K by applying the external magnetic of ±1000 G.

Results

In the polar and longitudinal MOKE measurements of Ni/Cu(001), we found that the SRT occurs at the critical Ni thickness of 9.0 ML before Cu capping and 7.0 ML after 2 ML Cu capping, implying the stabilization of perpendicular magnetic anisotropy (PMA). On the contrary, for the Ni/O/Cu(001), the SRT occurs at the critical Ni thickness of 5.5 ML before Cu capping and 7.0 ML after 2 ML Cu capping, indicating the instabilization of PMA.

In order to obtain structural information on these two kinds of films, the Auger electron spectra and the LEED pattern were observed. The oxygen atoms are found to act as a surfactant and locate always at the surface even after Ni and Cu deposition. Combining the MOKE and Auger results, we can conclude that the surface oxygen atom stabilizes PMA more effectively than the surface Cu atom.

For the understanding of such magnetic anisotropy, we have performed Ni L-edge XMCD. Figure 1 shows the XMCD spectra. In the 5.5 ML Ni film on clean Cu(001), the L_{III}-edge XMCD signals are gradually suppressed with the Cu capping, while in the 11 ML Ni film, the XMCD intensity is almost constant. This results indicate that with the Cu capping the orbital magnetic moments are reduced along the in-plane direction and not along the surface normal direction. On the contrary, in the 4.8 ML Ni film on O/Cu(001), the L_{III}-edge XMCD signals are gradually increased, implying the enhancement of the orbital magnetic moment.

Figure 2 shows the orbital magnetic moment (m_l) and the hysteresis loss (*BH*) obtained the present XMCD and MOKE measurements, respectively. It is clearly found that these quantities behave very similar.

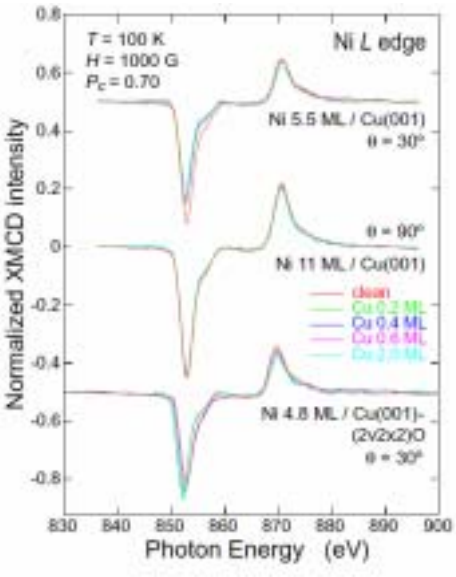

Fig. 1 Ni L-edge XMCD of 5.5 ML Ni on clean Cu(001) (always in-plane magnetized; measured at grazing x-ray incidence of 30°), 11 ML Ni on clean Cu(001) (always perpendicularly magnetized; measured at normal x-ray incidence), and 4.8 ML Ni on O/Cu(001) (always in-plane magnetization; measured at grazing x-ray incidence of 30°).

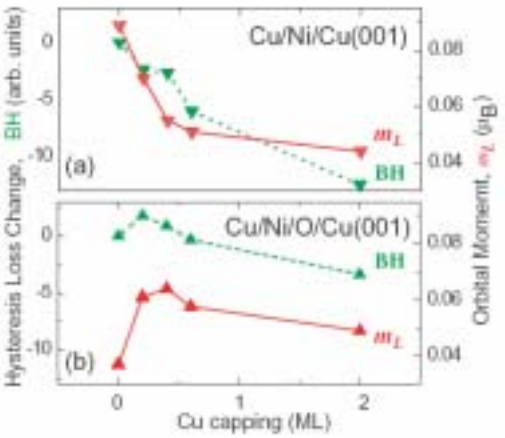

Fig. 2 Hystetesis loss and orbital magnetic moments of the Cu-capped Ni films on clean and O-preadsorbed Cu(001) as a function of Cu coverage.

[1] T. Nakagawa *et al.*, UVSOR Activity Report 2003 (2004) 39.

BL4B

Spin Reorientation Transition in Ag-Covered Co Films Grown on Vicinal Cu(001) Surface

T. Nakagawa, H. Watanabe, T. Yokoyama

Department of Molecular Structure, Institute for Molecular Science, Okazaki 444-8585 Japan

Magnetic thin films grown on vicinal surfaces exhibit strong uniaxial magnetic anisotropy; the magnetic property should be essentially different between the step-parallel and perpendicular directions. In this work, in order to obtain microscopic information on the spin reorientation transition in Ag-deposited Co films on Cu(1 1 17), we performed the longitudinal magneto-optical Kerr effect (L-MOKE) and the x-ray magnetic circular dichroism (XMCD) experiments.

Experiments

6 monolayer (ML) Co was deposited on clean Cu(1 1 17) at room temperature in ultrahigh vacuum chambers. The Co thickness was monitored with the RHEED oscillations. Ag was subsequently deposited on Co/Cu(1 1 17). Co *L*-edge XMCD was taken at BL4B at a temperature of ~100 K and at grazing x-ray incidence of 30° by applying the external magnetic of ±1000 G.

Results

Figure 1 shows the magnetic hysteresis loops of L-MOKE. In the clean Co film, the magnetization curve along the //step direction exhibits normal rectangular shape, while that along the ⊥step direction shows a double loop with zero remanence, this implying the easy axis of the //step direction. On the contrary, the reverse is true for the 0.2 ML Ag-deposited Co film; the magnetic easy axis changes from //step to ⊥step, exhibiting clear spin reorientation transition. This results is identical with the previous report by Weber *et al*. [1].

Figure 2 shows the Co L-edge XMCD. The intensities of the L_{III}- and L_{II}-edge peaks exhibits clear difference between the clean and Ag-deposited Co films. The sum-rule results are given in Table 1. Although the difference is rather small, one can find that a larger orbital magnetic moments give the magnetic easy axis.

Moreover, we have determined the inclination angle of the easy axis. Figure 3 shows the results of the XMCD variation. The *x*-intercept corresponds to the easy axis, where 0° and –4.8° respectively mean parallel to the physical plane and to the terrance plane. The present finding in Fig. 3 concludes that the Ag deposition induces also the out-of-plane rotation of the easy axis from the physical surface plane (0°) to the terrance plane (–4.8°).

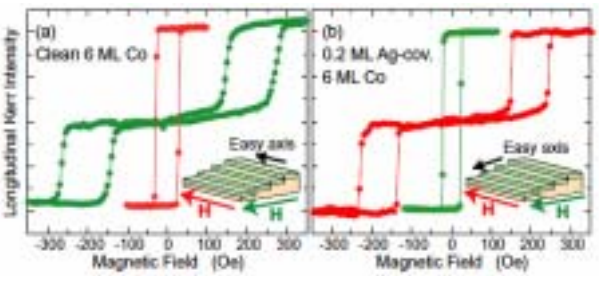

Fig. 1 L-MOKE hysteresis loops of (a) clean and (b) Ag-deposited 6 ML Co/Cu(1 1 17) at 100 K.

Table 1 The results of the sum-rule analysis for 6 ML Co on Cu(1 1 17). The spin (m_s) and orbital (m_l) magnetic moments of Co are given.

	direction	m_l (μ_B)	m_s (μ_B)
Clean	// step	0.246	1.526
	⊥step	0.225	1.474
0.2 ML Ag dep.	// step	0.200	1.468
	⊥step	0.218	1.485

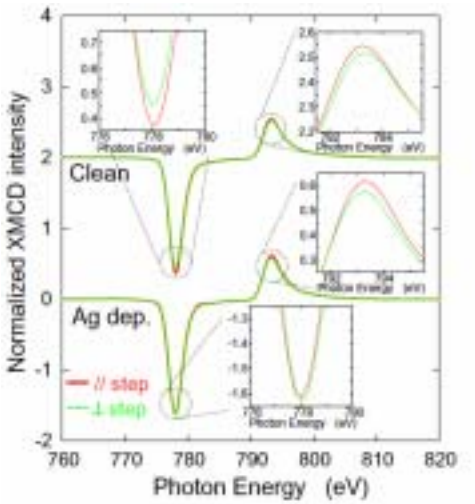

Fig. 2 Co L-edge XMCD of 6 ML Co/Cu(1 1 17) at 100 K before and after 0.2 ML Ag deposition.

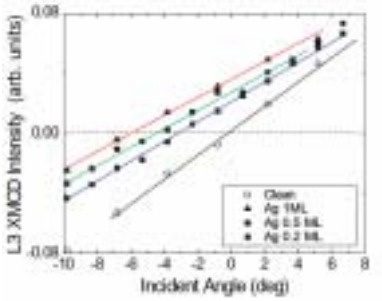

Fig. 3 Angle dependence of Co L_{III}-edge XMCD intensity of 6 ML Co/Cu(1 1 17).

[1] Weber *et al*., Phys. Rev. **B52** (1995) R14400.

BL4B

Drastic Magnetization Change Observed in NO Adsorption on Co/Cu(1 1 17)

T. Nakagawa, H. Watanabe, T. Yokoyama

Department of Molecular Structure, Institute for Molecular Science, Okazaki 444-8585 Japan

Magnetic thin films grown on vicinal surfaces exhibit strong uniaxial magnetic anisotropy and the anisotropy could be modified by surface chemical treatments. In this work, we have investigated the effect of NO adsorption on uniaxial Co films grown on Cu(1 1 17) by means of the longitudinal magneto-optical Kerr effect (L-MOKE) and the x-ray magnetic circular dichroism (XMCD) experiments.

Experiments

6 monolayer (ML) Co was deposited on clean Cu(1 1 17) at room temperature in ultrahigh vacuum chambers. The Co thickness was monitored with the RHEED oscillations. The Co film was exposed to 1 L NO to give a saturated ~0.5 ML adsorption state of NO/Co/Cu(1 1 17). Co *L*-edge XMCD was taken at BL4B at a temperature of ~100 K and at grazing x-ray incidence of 30 by applying the external magnetic of 1000 G.

Results

Figure 1 shows the magnetic hysteresis loops of L-MOKE. In the clean Co film, the magnetization curve along the //step direction exhibits normal rectangular shape, while that along the step direction shows a double loop with zero remanence, this implying the presence of strong uniaxial magnetic anisotropy and the easy axis of the //step direction. However, drastic changes can be seen after NO adsorption. The coercivity is reduced noticeably, and the //step and step loops are completely identical, this indicating the disappearance of the inherent uniaxial anisotropy and the appearance of almost fourfold symmetric magnetic anisotropy. Such a change is much more drastic than the film on flat Cu(001), as shown in Fig. 2.

Figure 2 shows the Co L-edge XMCD. The intensities of the L_{III}- and L_{II}-edge peaks exhibits clear difference between the clean and NO-adsorbed Co films. The sum-rule results are given in Table 1. Although the difference is rather small, one can find that in a clean Co film a larger orbital magnetic moments give the magnetic easy axis, while the orbital magnetic moments are essentially the same between the //step and step directions after NO adsorption. This is consistent with the L-MOKE results.

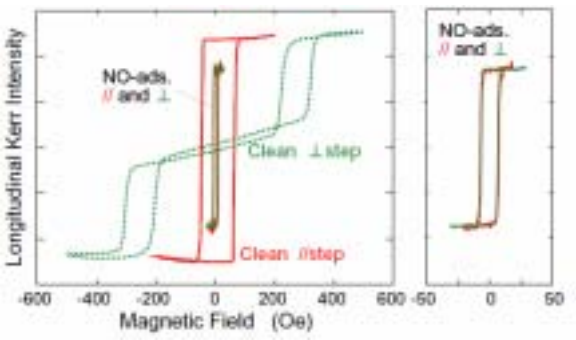

Fig. 1 L-MOKE hysteresis loops of clean and NO-adsorbed 6 ML Co films on Cu(1 1 17) at 100 K. The right figure is just the magnification along the *x* axis.

Table 1 The results of the sum-rule analysis for 6 ML Co on Cu(1 1 17). The spin (m_s) and orbital (m_l) magnetic moments of Co are given.

d	irection	m_l ($_B$)	m_s ($_B$)
Clean	// step	0.256	1.459
	step	0.224	1. 454
0.5 ML NO ads.	// step	0.116	0.866
	step	0.123	0. 879

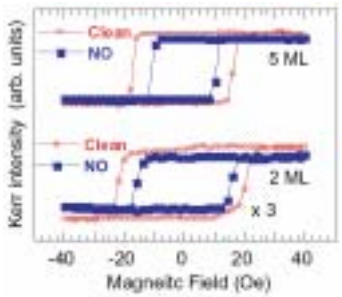

Fig. 2 L-MOKE hysteresis loops of clean (red) and NO-adsorbed (blue) 5 and 2 ML Co films on the flat Cu(001) surface.

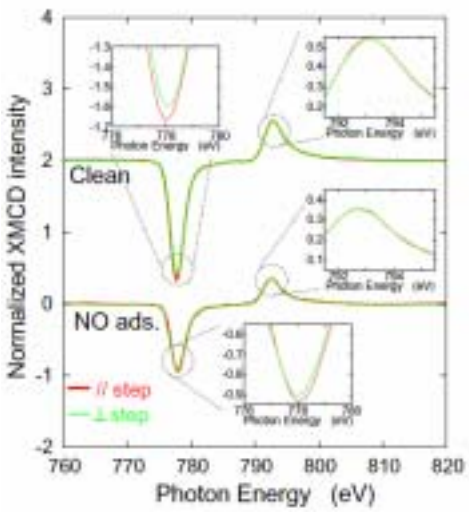

Fig. 3 Co L-edge XMCD of 6 ML Co/Cu(1 1 17) at 100 K before and after 0.5 ML NO adsorption.

BL4B

Enhancement of Magnetization of Fe/Cu(001) Induced by K Deposition

T. Nakagawa, H. Watanabe, T. Yokoyama

Department of Molecular Structure, Institute for Molecular Science, Okazaki 444-8585 Japan

It is interesting to investigate whether electron donation to magnetic metal films induces the enhancement or suppression of magnetization. In the present work, we have studied the effect of K adsorption on *fct* Fe grown on Cu(001) by means of the polar magneto-optical Kerr effect (P-MOKE) and the x-ray magnetic circular dichroism (XMCD) methods.

Experiments

3 monolayer (ML) Fe was deposited on clean Cu(001)-(1×1) at room temperature in ultrahigh vacuum chambers. Special care was taken of good vacuum because of easy oxidation of K. The thickness was monitored with the RHEED oscillations. K was subsequently deposited on Fe/Cu(001). Fe *L*-edge XMCD was taken at BL4B [1] at a temperature of ~100 K and at normal x-ray incidence (the films shows perpendicular easy axis) by applying the external magnetic of ±1000 G. For comparison, Co L-edge XMCD was examined for K/Co(3ML)/Cu(001) at grazing x-ray incidence.

Results

Figure 1 shows the P-MOKE intensity as a function of K coverage, which was measured during K deposition. With the increase in the K coverage, the P-MOKE intensity increases and at 0.1 ML K deposition it is maximized. More deposition leads to the suppression. The K coverage of 0.1 ML roughly corresponds to the work function minimum.

Although the MOKE intensity is usually proportional to the magnetization, it could not be the case if the electronic structure changes drastically. In order to confirm the enhanced magnetization and to obtain more direct information, we have performed XMCD measurements. Figure 2 shows the Fe L-edge XMCD. A small increase in the XMCD signals is actually found at the K coverage of 0.1 ML.

The results of the sum-rule analysis are summarized in Table 1, together with those of K/Co/Cu(001). In both the Fe and Co cases, the number of 3*d* holes, which was estimated from the intensity of the white lines, is gradually reduced with the K coverage, this exemplifying the electron donation from K. In the Co case, the spin magnetic moment decreases monotonically with the K coverage. This finding is reasonable since the majority 3*d* band of fcc Co is fully occupied and the donated electron is transferred to the minority 3*d* bands, leading to the reduction of the spin magnetic moment of Co. On the contrary, the spin magnetic moment of Fe is maximized at 0.1 ML K. This verifies that the Fe spin magnetic moment is enhanced by a small amount of K deposition.

Table 1 The results of the sum-rule analysis for 3 ML Fe and Co on Cu(001). 3*d* hole numbers and spin and orbital magnetic moments of Fe and Co are given.

	K dep. (ML)	$3d_{hole}$ number	m_s (μ_B)	m_l (μ_B)
3 ML Fe /Cu(001)	0.0	3.40	2.29	0.24
	0.1	3.27	2.40	0.24
	0.2	3.00	1.91	0.17
3 ML Co /Cu(001)	0.0	2.50	1.67	0.26
	0.1	2.37	1.58	0.26
	0.2	2.27	1.50	0.29

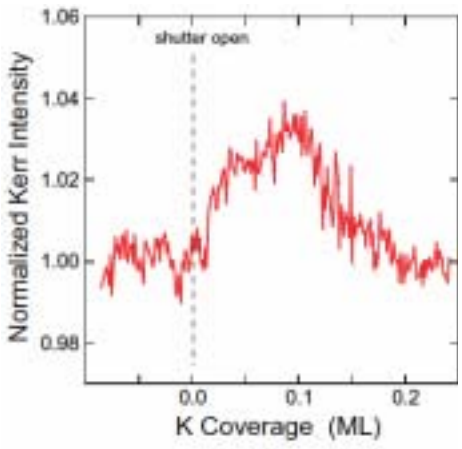

Fig. 1 P-MOKE intensity of 3 ML Fe/Cu(001) at 100 K as a function K deposition.

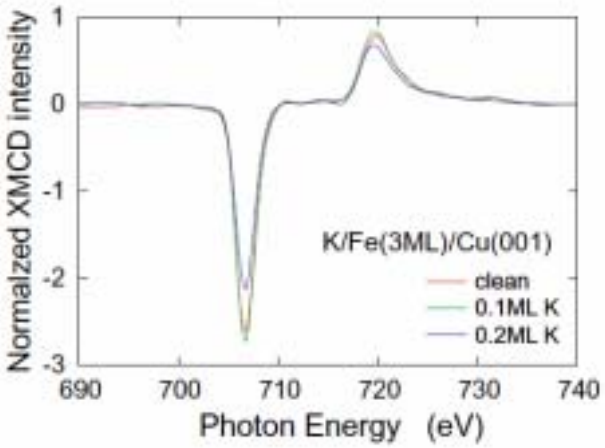

Fig. 2 Fe L-edge XMCD of 3 ML Fe/Cu(001) (perpendicularly magnetized) at 100 K for the K coverages of 0.0, 0.1 and 0.2 ML.

[1] T. Nakagawa *et al.*, UVSOR Activity Report 2003 (2004) 39.

BL5U

Absolute Asymmetric Synthesis of rac-Leucine in Ice at 21 K by Circularly Polarized Synchrotron Radiation: a Terrestrial Proof of the Origin of Homochirality in Biosphere

H. Nishino[1], M. Hosaka[2], M. Katoh[2], Y. Inoue[1]

[1]*Entropy Control, ICORP, Japan Science and technology Agency, Toyonaka 560-0085 Japan*

[2]*UVSOR facility, Institute for Molecular Science, Okazaki 444-8585 Japan*

The homochirality in biosphere is an extreme case of the entropy control in nature, while the origin of biomolecular homochirality is one of the most controversial issues in the chemical evolution on Earth [1]. It is proposed that the enantiomeric enrichment can be achieved by the circularly or elliptically polarized synchrotron radiation from a neutron star. This idea is supported by the finding of optically active amino acids in the organic mantle of the Murchison meteorite [2]. For this hypothesis, we have already reported the absolute asymmetric synthesis (AAS) of some aliphatic amino acids in aqueous solutions at varying pH (defined at 298 K), by using left- and right-handed circularly polarized light (*l*- and *r*-CPL) proceeded irrespective of the solution pH through different mechanisms [3].

In outer space, amino acids are thought to be frozen in icy carbonaceous chondrite meteorite. Recently, it was shown that a variety of racemic amino acids are photochemically produced indeed from a low-temperature matrix (12-15 K) of H_2O, CH_3OH, CO_2, CO, and NH_3 (2:1:1:1:1), which mimics the icy meteorite condition in outer space [4]. Hence, to fill the missing link of the origin of the homochirality in biomolecules, it is essential to examine whether the AAS of amino acids by CPL proceeds in an ice matrix or not. In this study on the AAS of leucine (Leu) in ice, we irradiated the icy samples at 21 K (ice **XI**) and 81 K (ice **Ih**) with the 215 nm *l*- and *r*-CPL, generated by a helical undulator installed in the electron storage ring UVSOR-II.

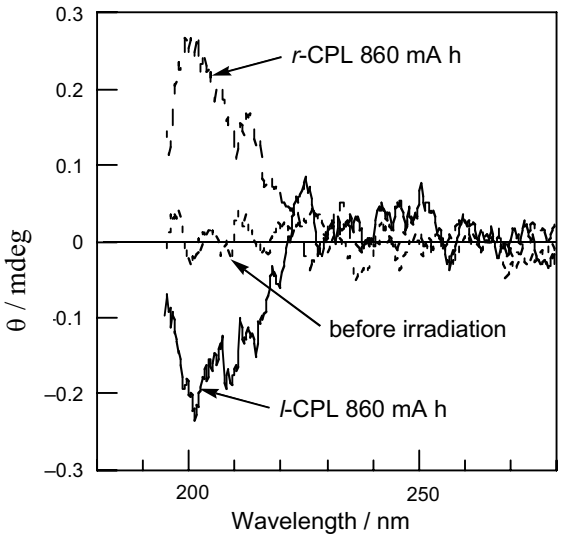

Fig. 1 The final CD of *rac*-Leu [*rac*-Leu]$_0$ = 6.5 mM, $pH_{25°C}$ = 7) irradiated at 215 nm by CPL (21 K). % Decomposition: *r*-CPL 860 mA h; 20.8%, *l*-CPL 860 mA h; 17.4%. Path length of CD cell: 0.2 cm.

We verified for the first time the occurrence of AAS of Leu even at 21 K by using circular dichroism (CD) spectroscopy (Figure 1). Quantitative product analyses of the irradiated samples revealed that, irrespective of the original pH (defined at 298 K), ammonia and isovaleraldehyde are the only detectable products from icy Leu irradiated at 215 nm. This is the first clear observation that the photodecomposition of Leu does occur even in a 21 K ice through photodeamination, which requires less molecular motions. In ice, HCl does not dissociate to an ion pair [H^+ + Cl^-], but exists as molecule at 77 K [5]. Hence, irrespective of the original pH defined at 25 °C, Leu exists as a zwitterion at 21 K. This may rationalize the very similar photochemical behavior of Leu in ice of different original pHs of 1 and 7.

These results unambiguously complete the whole scenario that, in outer space, simple starting materials, such as H_2O, CH_3OH, CO_2, CO, and NH_3, are irradiated by polarized or unpolarized VUV-UV irradiations to produce a mixture of racemic amino acids, including some of the essential amino acids [4], which in turn are enantioselectively photodecomposed on the way to Earth by the circularly polarized radiation from a neutron star or a star-forming area.

[1] W. A. Bonner, Origins Life Evol. Biosphere **21** (1991) 59.

[2] J. R. Cronin and S. Pizzarello, Science **275** (1997) 951.

[3] H. Nishino, A. Kosaka, G. A. Hembury, F. Aoki, K. Miyauchi, H. Shitomi, H. Onuki and Y. Inoue, J. Am. Chem. Soc. **124** (2002) 11618.

[4] M. P. Bernstein, J. P. Dworkin, S. A. Sandford, G. W. Cooper, L. J. Allamandola, Nature **416** (2002) 401. G. M. Munoz Caro, U. J. Meierhenrich, W. A. Schutte, B. Barbler, A. A. Segovia, H. Rosenbauer, W. H. P. Thiemann, A. Brack and J. M. Greenberg, Nature **416** (2002) 403.

[5] H. Kang, T.-H. Shin, S. -C. Park, I. K. Kim and S. -J. Han, J. Am. Chem. Soc. **122** (2000) 9842.

BL7U

Undulator Radiation Induced Si-H Dissociation on H-Si(111) Surfaces Observed by STM

Y. Nonogaki, T. Urisu

Dept. Vaccum UV Photoscience, Institute for Molecular Science, Okazaki 444-8585 Japan

Synchrotron-radiation-stimulated reactions, such as SR-etching and photon-stimulated desorption, have been attractive subjects from the view points of not only engineering but also surface science, due to their interesting characteristics of unique material and site selectivity, high spatial resolution and low damage.

We designed and constructed the undulator beamline equipped with an STM observation system at the UVSOR to investigate the excitation-energy dependence of SR-stimulated reactions. The undulator emits the quasi-monochromatized and tunable light of 50 - 120 eV, which is suitable for excitation of the Si 2p (~100 eV). In this study, the irradiation effects and its excitation energy dependence on the H-Si (111) surfaces were investigated by in-situ STM. Although photon-stimulated H desorptions from H-Si (111) surfaces have been studied by detecting the desorbing molecules[1,2], there is no report with the surface morphology studied by STM after the photon-stimulated desorption.

The clean Si (111) surface was exposed to atomic H at 350°C for 10 min, which gives sufficiently wide 1x1 areas. The surface was irradiated by the undulator emission with irradiation dose of 5,000 and 10,000 mA sec (ring current x exposure time) at room temperature. The undulator gap height was fixed at 17 mm, 20 mm and 25 mm.

Figure 1 (a) shows a 10 nm x 10 nm STM image of the H-Si (111) surface obtained by the 10 min atomic H exposure at 350°C. Islands and small protrusions (SPs) are visible on a flat surface with the atomic corrugation, as reported in Refs. 3 and 4. The flat surface with the atomic corrugation consists of rest-atom monohydrides. According to Ref. 4, the SPs are assigned to isolated adatom trihydrides or rest-atoms with missing H. The SP density is observed to be 1.5%ML.

Figure 1(b) shows the H-Si (111) surface after the undulator beam irradiation of 5,000 mA sec dose (1st harmonic radiation at ~84 eV). The number of the SPs significantly increased on the rest-atom monohydride surface from 1.4%ML to 4.5%ML. By increasing the exposure to 10,000 mA sec, the SP density increased to 12.8%ML, as shown in Fig. 1(c). The distribution of the SPs seems to be random and independent on the kind of the rest-atoms both on the faulted or unfaulted half of the 7x7 structure. It is most reasonable to assign the appeared SPs to the rest-atoms with missing H. This means that the rest-atom Si-H bond is easily dissociated by the irradiation of 84 eV photons.

The undulator gap height was changed to investigate the dependence of the SP density on the incident photon energy. The irradiation dose was fixed at 5,000 mAsec. The peak energies of the 1st harmonic radiation were changed from 68 eV to 113 eV by varying the gap height from 17 mm to 25 mm.

It is found that the SP densities observed in the 38 nm x 38 nm STM images were depend not on Si 2p core electron transition threshold but on total photon flux irradiated to the surface. From these results, it is concluded that the main mechanism of the H desorption from the rest-atom monohydrides is the direct valence electron excitations by the undulator beam photons.

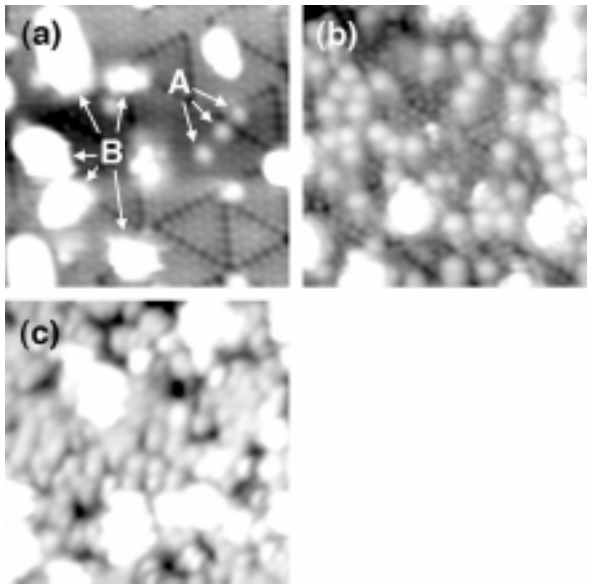

Fig. 1 10 nm x 10 nm STM images of H-Si (111) surfaces after the undulator beam irradiations with the exposure of (a) 0 mAsec, (b) 5,000 mAsec and (c) 10,000 mAsec. In (a), small protrusions (SPs) and adatom islands (AIs) are indicated by A and B, respectively. It is observed that the SP density significantly increases with increasing irradiation dose. The appeared SPs are assigned to the rest-atoms with missing H.

[1] M.L. Knotek and G.M. Loubriel, R.H. Stulen, C.E. Parks, B.E. Koel, and Z. Hussain, Phys. Rev. B **26** (1982) 2292.

[2]H. Akazawa, M. Sugiyama, S. Maeyama, M. Oshima and Y. Watanabe, Phys. Rev. B **57** (1998) 4883.

[3] J.J. Boland, Surf. Sci. **244** (1991) 1.

[4] F. Owman and P. Mårtensson, Surf. Sci. **324** (1995) 221.

BL8A

Synchrotron Radiation-Excited Etching of ZnTe

T. Tanaka, Y. Kume, K. Hayashida, K. Saito, M. Nishio, Q. Guo, H. Ogawa
Saga University, 1 Honjyo, Saga 840-8502, Japan

Synchrotron radiation (SR) is an ideal light source for the photo-excited processes because of its high intensity, small divergence, and continuity of the wavelength from the x-ray to the infrared. With respect to the SR-excited etching, the materials for an integrated circuit such as Si, SiO_2, *etc.*, have been studied actively [1]. However, few papers concerning the etching of the compound semiconductor materials such as III-V and II-VI semiconductors have been published to date in spite of their importance in the optoelectronic application. Since the single crystal films of II-VI semiconductors, *e.g.* ZnTe, can be grown by SR-excited growth [2], the development of the SR-excited etching is an important next step to make the electronic devices. Recently, we demonstrated the possibility of the SR-excited etching of ZnTe using Ar gas [3]. In this study, we have investigated the effect of the pressure upon the SR-excited etching process of ZnTe using Ar gas.

Experiments

The irradiation experiments were performed at a beam line, BL-8A, in UVSOR facility at IMS. The critical energy of the SR from the bending magnet field of the 750 MeV electron storage ring is 425 eV. The undispersed SR was focused on a sample in a reaction chamber using a Pt-coated toroidal mirror. The light intensities on the sample measured using an Au diode were determined as about 2×10^{16} photons/s at a stored current of 100 mA. The Ar pressure was changed between 0.02 and 0.5 Torr. The SR was irradiated perpendicularly to the surface of ZnTe (100) at room temperature through a Ni mesh mask of 100 lines/in. and 80% transmittance. The Ni mesh mask was put on the surface of the ZnTe directly. The ZnTe and the Ni mesh were negatively biased against the reaction chamber. The bias voltage was kept at –80 V in all experiments.

Results and discussion

The pattern of the Ni mask was transferred to the surface of the ZnTe exactly. However, the etched area was found to extend beyond the calculated beam size. It was also found that the etched depth depends on the photon flux density. The maximum etched depth is about 600 nm for 7×10^4 mA·min at 0.05 Torr. The dependence of the etching rate of ZnTe on the pressure is shown in Fig. 1. The etching rate is increased with increasing the pressure. In this experiment, the maximum etching rate is 16.7 nm/A·min, which is obtained at the pressure of 0.2 Torr.

In order to discuss the etching mechanism, we have also carried out the experiments using LiF window. LiF window pass through the photons with the energy lower than about 12 eV. Although the SR was irradiated to the sample through the window for 10^5 mA·min at the pressure of 0.05 Torr under the same bias condition, the ZnTe was not etched at all. This indicates that the photons with energy less than 12 eV does not play important roles in the etching process. The photoabsorption cross section of Ar is reported to be almost zero in the energy range below the absorption edge of the LiF window, whereas it is quite large in the energy range between 12 eV and 50 eV [4]. The first ionization energy of Ar is 15.76 eV. We suspect that the ionization of Ar is necessary in this etching process. Since the mean free path of Ar is estimated to be around 1 mm at the pressure of 0.05 Torr, a part of Ar ions extends to the outside of the beam, resulting in the further expansion of the etching area. The increase of Ar gas pressure leads to the increase of Ar^+ ion density, and consequently, the etching rate is increased according to the gas pressure.

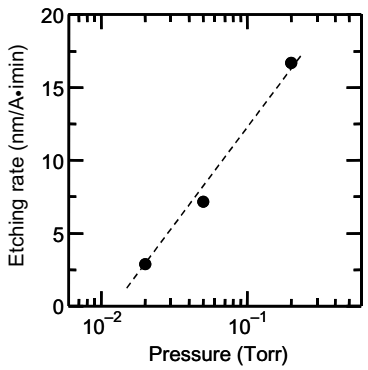

Fig. 1 Dependence of the etching rate of ZnTe on the pressure.

[1] D. C. Mancini, S. Varma, J. K. Simons, R. A. Rosenberg, and P. A. Dowben, J. Vac. Sci. Technol. B **8** (1990) 1804.
[2] T. Tanaka, K. Hayashida, S. Wang, Q. Guo, M. Nishio, and H. Ogawa, Nucl. Instr. And Meth. B **199** (2003) 356.
[3] T. Tanaka, Y. Kume, S. Tokunaga, K. Hayashida, M. Nishio, Q. Guo, and H. Ogawa, AIP series of conference proceedings **705** (2004) 1154.
[4] W. F. Chan, G. Cooper, X. Guo, G. R. Burton, and C. E. Brion, Physical Review A **46** (1992) 149.